Anal. Chem. **2006,** *78,* 3807−3814

Detection of Explosives and Explosives-Related Compounds by Single Photon Laser Ionization Time-of-Flight Mass Spectrometry

Christopher Mullen, Amos Irwin,† Bethany V. Pond,‡ David L. Huestis, Michael J. Coggiola, and Harald Oser*

Molecular Physics Laboratory, SRI International, Menlo Park, California 94025

The application of single photon ionization in combination with mass-selective detection by time-of-flight mass spectrometry is described for the rapid detection of the nitro-containing explosives and explosives-related compounds nitrobenzene, 1,3-dinitrobenzene, *o*-nitrotoluene, 2,4-dinitrotoluene, and 2,4,6-trinitrotoluene, as well as the peroxide-based explosive triacetone triperoxide in the gas phase. The technique is demonstrated to be a plausible approach for laser-based rapid detection of explosives. The limits of detection for nitrobenzene and 2,4-dinitrotoluene using SPI were also measured and determined to be 17−24 (S/N ∼2:1) and ∼40 ppb (S/N ∼2:1), respectively.

Recent world events have increased the interest in the detection of explosives and explosives-related compounds (ERCs) with a low false alarm rate, whether as a preventive measure to detect improvised explosive devices (IEDs), to screen airport passengers, or to discover unexploded ordinance in a battlefield situation.The detection of nitro-containing explosives, such as trinitrotoluene (TNT), RDX, and HMX, and ERCs in the gas phase is challenging due to their low vapor pressure and the inherent instability of the parent compounds. When this class of explosives is left in the environment for a long period of time, such as when buried in a landmine, they degrade into a variety of species, which include nitrobenzene (NB), dinitrobenzene (DNB), and nitrotoluene (NT).[1,2] Fortunately, some of these degradation products have significantly higher vapor pressures, thus increasing the ease with which they can be detected in the gas phase.

To successfully detect explosives and ERCs, a rapid, selective, and sensitive device needs to be developed. Such a device must be capable of accurately determining the presence of explosives or ERCs in order, for example, to reduce the false positive and negative detection rates.

Despite the widespread deployment of ion mobility-based detection systems[3−5] for nitro-containing explosives, particularly as a screening tool at commercial airports, the technology is not universally applicable to the detection of all classes of ERCs and false negative and positive detection rates are problematic. However, several other methods for the detection of explosives have been studied and developed. Specifically, mass spectrometer-based methods have shown the most promise for identifying explosives in trace amounts.

Electrospray ionization in negative ion mode[6−8] and atmospheric pressure chemical ionization[9] have been widely used for the detection of explosives in liquid solutions. Additionally, chemical ionization Fourier transform ion cyclotron resonance mass spectrometry has been employed for the detection of explosives in the gas phase using the trimethylsilyl cation.[10,11]

Gas chromatography-based methods in combination with electron capture detectors[1] or with mass-selective detection[12] have been successfully applied for the gas-phase analysis of explosives.

Current explosives vapor detection methods generally require preconcentration prior to analysis, due to the low vapor pressures of most explosives and explosives-related compounds[13,14] and the relative lack of sensitivity of the instrumentation. This increases the detection time due to the sample adsorption and subsequent desorption steps.

Laser-based ionization techniques combined with mass spectrometry have been shown to have unique properties for chemical analysis that make them applicable to this problem. In particular, this combination exhibits sufficient sensitivity and selectivity that preconcentration and pretreatment of the analyte may not be required.

* Corresponding author. E-mail: harald.oser@sri.com.
† Present address: Amherst College, Amherst, MA 01002.
‡ Present address: Varian Inc., Walnut Creek, CA 94598.

(1) Walsh, M. E. *Talanta* **2001**, *54*, 427−438.
(2) Jenkins, T. F.; Leggett, D. C.; Miyares, P. H.; Walsh, M. E.; Ranney, T. A.; Cragin, J. H.; George, V. *Talanta* **2001**, *54*, 501−513.
(3) Tam, M.; Hill, H. H. *Anal. Chem.* **2004**, *76*, 2741−2747.
(4) Lawrence, A. H.; Neudorfl, P. *Anal. Chem.* **1988**, *60*, 104−109.
(5) Ewing, R. G.; Miller, C. J. *Field Anal. Chem. Technol.* **2001**, *5*, 215−221.
(6) Wu, Z. G.; Hendrickson, C. L.; Rodgers, R. P.; Marshall, A. G. *Anal. Chem.* **2002**, *74*, 1879−1883.
(7) Yinon, J.; McClellan, J. E.; Yost, R. A. *Rapid Commun. Mass Spectrom.* **1997**, *11*, 1961−1970.
(8) Zhao, X. M.; Yinon, J. *J. Chromatogr., A* **2002**, *977*, 59−68.
(9) Song, Y. H.; Chen, H.; Cooks, R. G. *Rapid Commun. Mass Spectrom.* **2005**, *19*, 3493−3499.
(10) Crellin, K. C.; Dalleska, N.; Beauchamp, J. L. *Int. J. Mass Spectrom.* **1997**, *165*, 641−653.
(11) Crellin, K. C.; Widmer, M.; Beauchamp, J. L. *Anal. Chem.* **1997**, *69*, 1092−1101.
(12) Barshick, S. A.; Griest, W. H. *Anal. Chem.* **1998**, *70*, 3015−3020.
(13) Yinon, J. *Trends Anal. Chem.* **2002**, *21*, 292−301.
(14) Yinon, J. *Forensic and Environmental Detection of Explosives*; John Wiley: New York, 1999.

10.1021/ac060190h CCC: $33.50
Published on Web 04/21/2006

Laser ionization of explosives and ERCs has been studied extensively using nanosecond duration laser pulses.[15−20] These compounds were ionized in the nanosecond regime using resonance enhanced multiphoton ionization (REMPI) and detected through either laser-induced fluorescence (LIF) or time-of-flight mass spectrometry (TOF-MS). The first reported work was by Marshall et al., who proposed the generally accepted fragmentation mechanism of the nitro-containing explosives and ERCs following excitation of the parent molecule using a nanosecond laser pulse.[15] The process from excitation to detection is as follows: Upon initial nanosecond laser excitation, the parent molecule fragments on a time scale of ~100 fs, resulting in the release of NO_2 and other ERC byproducts. Next, the NO_2 fragment absorbs additional photons and is excited to a predissociative state, resulting in the formation of NO and O. The NO fragment then undergoes subsequent photon absorption, resulting in a REMPI process through the A−X (0−0, 0−1, or 0−2) electronic transition from the ground state ($X\ ^2\Pi$) to the first excited state ($A\ ^2\Sigma^+$), and the NO^+ ion is detected using TOF-MS. The entire process occurs within a single nanosecond laser pulse. In general, the laser ionization mass spectra of these species are dominated solely by the NO^+ ion with a wavelength dependence attributable to the A−X electronic transition in NO. Consequently, we initially investigated detection strategies based on the laser production of NO^+.

However, when the spectral excitation signatures of NO^+ arising from the fragmentation of TNT were compared with the NO^+ spectral features from fragmentation of nitromethane, no major difference could be found. This indicates that nanosecond REMPI may not be a suitable detection strategy for distinguishing TNT from background nitro compounds. As a result, to detect explosives and ERCs by applying laser ionization mass spectrometry, the ion signal, corresponding to either the specific fragment or the parent molecular ion must be observable.

Knowledge that the time scale for fragmentation of the explosives and ERCs is on the order of 100 fs led to the exploration of detection schemes using multiphoton ionization (MPI) employing ultrafast laser pulses.[21,22] In this scheme, two or more photons from an ultrashort pulse laser are used to ionize the parent molecule directly from the ground state. In this case, the femtosecond laser pulse duration is on the time scale of the fragmentation process, and as a result, the parent molecule ionizes before extensive fragmentation occurs. The lack of a resonant intermediate step is also an advantage over the REMPI scheme because many of the spectroscopic restrictions based on the intermediate-level location are removed. Another approach demonstrated by Ledingham et al., employed to detect nitroaromatic compounds, was the use of ultrafast MPI at 800 nm following nanosecond laser desorption of solid samples at 266 nm. Under these conditions, the parent molecular ion of trinitrobenzene (TNB) and TNT along with extensive fragmentation products were detected.[23]

Ultrafast MPI TOF-MS has also been reported without the use of laser desorption.[24,25] The fragmentation of the isomers of NT, dinitrotoluene (DNT), and TNT were extensively studied at wavelengths of 412 and 206 nm,[24] yielding results similar to that of the Ledingham studies.[21−23] Additionally, isomer-specific detection after MPI at 412 nm for two isomers of DNT was demonstrated.[25]

While the ultrafast approach was successfully shown to selectively ionize explosives and ERCs, the technique still may not be the most suitable for application to field scenarios due to the very delicate, complex, and hard to maintain laser system. Therefore, alternate laser-based ionization methods may prove more suitable to the field detection of explosives and ERCs.

A more robust laser-based ionization method is single photon ionization (SPI). This approach does not involve resonant excitation of an intermediate state, and the parent molecule is directly ionized using a vacuum ultraviolet (VUV) photon. VUV photons with a wavelength of 118.2 nm, or a photon energy of 10.49 eV, can easily and reliably be generated by frequency tripling the third harmonic output (354.6 nm) of a Nd:YAG laser in xenon.[26−28] The limited ionization energy provides a selective and efficient ionization method, since bulk gases such as nitrogen, oxygen, and water are not ionized, while most organic compounds are efficiently ionized. Previous studies have shown that almost no fragmentation of the parent molecule occurs because the excess ionization energy is minimal.[29−32] The ions generated via a SPI process are detected using a TOF mass spectrometer in the same manner used in other laser-based ionization approaches. SPI-TOF-MS has been successfully used in the detection of compounds present in the headspaces of tobacco smoke and gasoline, as well as common organic atmospheric pollutants, such as benzene, toluene, and xylene.[33,34] The ability to differentiate different types of alkanes,

(15) Marshall, A.; Clark, A.; Jennings, R.; Ledingham, K. W. D.; Sander, J.; Singhal, R. P. *Int. J. Mass Spectrom. Ion Processes* **1992**, *116*, 143−156.
(16) Lemire, G. W.; Simeonsson, J. B.; Sausa, R. C. *Anal. Chem.* **1993**, *65*, 529−533.
(17) Kosmidis, C.; Marshall, A.; Clark, A.; Deas, R. M.; Ledingham, K. W. D.; Singhal, R. P. *Rapid Commun. Mass Spectrom.* **1994**, *8*, 607−614.
(18) Marshall, A.; Clark, A.; Ledingham, K. W. D.; Sander, J.; Singhal, R. P.; Kosmidis, C.; Deas, R. M. *Rapid Commun. Mass Spectrom.* **1994**, *8*, 521−526.
(19) Wu, D. D.; Singh, J. P.; Yueh, F. Y.; Monts, D. L. *Appl. Opt.* **1996**, *35*, 3998−4003.
(20) Shu, J.; Bar, I.; Rosenwaks, S. *Appl. Phys. B: Lasers Opt.* **2000**, *71*, 665−672.
(21) Ledingham, K. W. D.; Kilic, H. S.; Kosmidis, C.; Deas, R. M.; Marshall, A.; McCanny, T.; Singhal, R. P.; Langley, A. J.; Shaikh, W. *Rapid Commun. Mass Spectrom.* **1995**, *9*, 1522−1527.
(22) Kosmidis, C.; Ledingham, K. W. D.; Kilic, H. S.; McCanny, T.; Singhal, R. P.; Langley, A. J.; Shaikh, W. *J. Phys. Chem. A* **1997**, *101*, 2264−2270.
(23) Hankin, S. M.; Tasker, A. D.; Robson, L.; Ledingham, K. W. D.; Fang, X.; McKenna, P.; McCanny, T.; Singhal, R. P.; Kosmidis, C.; Tzallas, P.; Jaroszynski, D. A.; Jones, R.; Issac, R. C.; Jamison, S. *Rapid Commun. Mass Spectrom.* **2002**, *16*, 111−116.
(24) Weickhardt, C.; Tonnies, K. *Rapid Commun. Mass Spectrom.* **2002**, *16*, 442−446.
(25) Tonnies, K.; Schmid, R. P.; Weickhardt, C.; Reif, J.; Grotemeyer, J. *Int. J. Mass Spectrom.* **2001**, *206*, 245−250.
(26) Lipson, R. H.; Dimov, S. S.; Wang, P.; Shi, Y. J.; Mao, D. M.; Hu, X. K.; Vanstone, J. *Instrum. Sci. Technol.* **2000**, *28*, 85−118.
(27) Hepburn, J. W. In *Laser Techniques in Chemistry*; Myers, A. B., Rizzo, T. R., Eds.; John Wiley and Sons: New York, 1995; Vol. 23, pp 149−183.
(28) Lockyer, N. P.; Vickerman, J. C. *Laser Chem.* **1997**, *17*, 139−159.
(29) Schuhle, U.; Pallix, J. B.; Becker, C. H. *J. Vacuum Sci. Technol., A* **1988**, *6*, 936−940.
(30) Pallix, J. B.; Schuhle, U.; Becker, C. H.; Huestis, D. L. *Anal. Chem.* **1989**, *61*, 805−811.
(31) Koster, C.; Grotemeyer, J. *Org. Mass Spectrom.* **1992**, *27*, 463−471.
(32) Vanbramer, S. E.; Johnston, M. V. *J. Am. Soc. Mass Spectrom.* **1990**, *1*, 419−426.
(33) Muhlberger, F.; Zimmermann, R.; Kettrup, A. *Anal. Chem.* **2001**, *73*, 3590−3604.
(34) Muhlberger, F.; Hafner, K.; Kaesdorf, S.; Ferge, T.; Zimmermann, R. *Anal. Chem.* **2004**, *76*, 6753−6764.

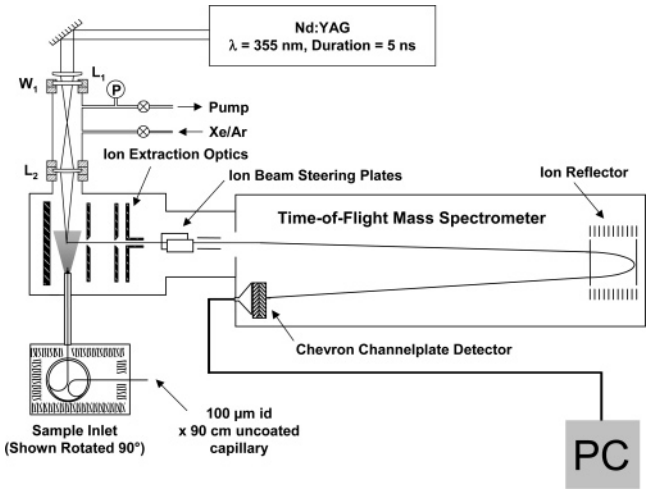

Figure 1. Schematic diagram of the SPI TOF-MS instrument.

alkenes, and aromatics in complex matrixes, such as gasoline and tobacco smoke, illustrates that the SPI-TOF-MS technique may be applicable to the detection of explosives and ERCs through headspace analysis, of landmines, for example.

The objective of our current research was to demonstrate the detection of explosives and ERCs by single photon ionization and determination of the limits of detection (LOD) for NB and 2,4-dinitrotoluene (2,4-DNT) in the gas phase.

EXPERIMENTAL SECTION

A detailed description of our laser ionization TOF-MS instrument is given elsewhere,[35] and therefore, only a brief summary is presented here (see Figure 1). The sample is introduced into the ionization region through a short length of deactivated capillary GC column that can be heated to 200 °C in order to accommodate the low vapor pressure of the samples. NB (Aldrich reagent grade, 99%), *o*-NT (Aldrich, ≥99%), triacetone triperoxide (TATP) (the TATP sample was synthesized at SRI International following the preparation described in the literature[36]), acetone (Aldrich Chromasolv, ≥99.8%), and hexane (Aldrich Reagent Plus, ≥99%) were delivered to the instrument at room temperature. Solid samples of 1,3-DNB (Aldrich, 97%), 2,4-DNT (Aldrich, 97%), and TNT (recrystallized from a commerical source, approximate purity ≥98%) were heated above their melting point, and the headspace above the samples was transferred to the instrument by heating the GC column and probe to the same temperature. The laser system consists of a Continuum Powerlite Precision 9010 Nd:YAG with a 5-ns pulse width, and a repetition rate of 10 Hz. The 118.2-nm light is produced by frequency tripling the third harmonic output (354.6 nm) of the Nd:YAG laser.[26] To accomplish this, the 354.6-nm laser beam (30 mJ pulse energy) is focused into a stainless steel tripling cell filled with Xe or Xe/Ar mixtures, which is attached directly to the ion source of the mass spectrometer using conflat flange hardware. W_1 and L_2 (Figure 1) act as vacuum breaks for the cell. A 120-mm fused-silica planoconvex lens (L_1 of Figure 1), yielding an estimated power density of 2.6×10^{12} W/cm^2 at the focus, was employed. The optimal cell pressure measured using a capacitance monometer (MKS Baratron), leading to maximum conversion efficiency, was found to be 20 Torr (Figure 2), by monitoring the benzene (78 amu) ion signal as a function of Xe pressure. An additional 35% more signal could be obtained using a ~7:1 mixture of Ar/Xe. A MgF_2 lens (f = 200 mm; L_2 of Figure 1) serves as the output window for the cell and also directs the 118.2-nm light into the ion source region. Since the residual 354.6-nm and product 118.2-nm beams copropagate and are spatially overlapped in the ion source, there is a chance that the overlap of the 118.2- and 354.6-nm beams could result in a 1 + 1 MPI process. As a result, it was desirable to evaluate the relative contribution of MPI to SPI resulting from the VUV photon source. This was accomplished using two methods; one by measuring the photoion signal as a function of input 354.6-nm energy into the tripling cell and also by photoionizing molecules (acetone, hexane, NB) with well-known photochemistries and energetics that would reveal the presence of a MPI process. Very little MPI was found (ratio MPI/SPI ~1.3×10^{-3}), and details of the analysis are reported in Results and Discussion.

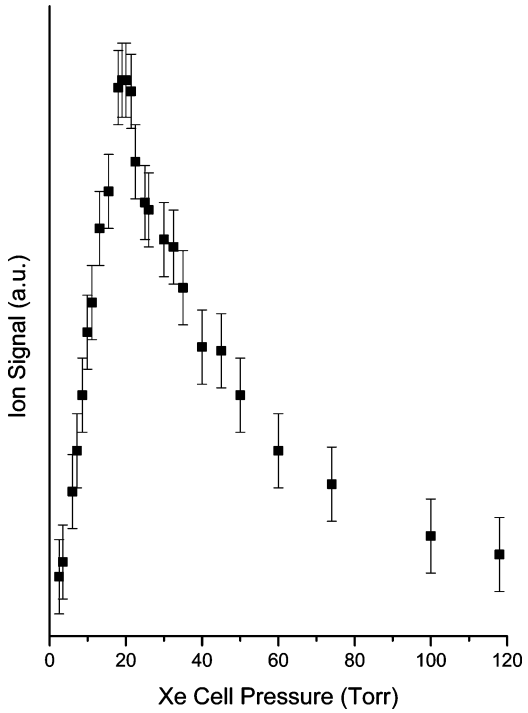

Figure 2. Plot of the benzene (78 amu) ion signal as a function of Xe gas pressure inside the VUV cell, used to optimize the third harmonic generation. 30 mJ of input 354.6-nm light was focused into the center of the cell with a 120-mm planoconvex lens, corresponding to an estimated power density of 2.6×10^{12} W/cm^2.

Ions produced by SPI are detected and mass analyzed using a compact reflectron time-of-flight mass spectrometer (Stefan Kesedorf, Munich, Germany) with a mass resolution of ~1000 ($m/\Delta m$), and recorded by a 1-GHz digitizer (Signatec, Corona, CA). Instrument control and data acquisition were performed by using custom in-house software based on the Labview (National Instruments, Austin, TX) programming environment.

Production of Known Analyte Concentrations for Calibration. The determination of the LOD for the ERCs was accomplished by attaching a VICI Metronics (Houston, TX) model 230 Dynacalibrator permeation tube-based system directly to the

(35) Oser, H.; Coggiola, M. J.; Faris, G. W.; Young, S. E.; Volquardsen, B.; Crosley, D. R. *Appl. Opt.* **2001**, *40*, 859−865.
(36) Wolffenstein, R. *Chem. Ber.* **1895**, *28*, 2265.

Table 1. Ionization Energies and Appearance Energies for the Explosives, ERCs, Acetone, and Hexane

molecule	IE (eV)[a]	mass peak (amu)	appearance energy (eV)	reaction	ref
ntirobenzene	9.94 ± 0.08	123			
		30	11.04 ± 0.05	$NO^+ + C_6H_5$	53
			10.89 ± 0.04		54
		51	11.40 ± 0.05	$C_4H_3^+ + NO + C_2H_2O$	53
		65	11.30 ± 0.05	$C_5H_5^+ + CO + NO$	53
			11.08 ± 0.16		54
		77	11.14 ± 0.05	$C_6H_5^+ + NO_2$	53
			11.08 ± 0.16		54
		93	10.98 ± 0.05	$C_6H_5O^+ + NO$	53
			10.89 ± 0.04		54
1.3-dinitrobenzene	10.4	168			
		122	12.3	$C_6H_4NO_2 + NO_2$	41
o-nitrotoluene	9.24	137			
		120	≤9.69	$C_7H_6NO^+ + OH$	57
2.4-dinitrotoluene	na[b]	182	na		
2,4,6-trinitrotoluene	10.59 ± 0.04	227	na		58
triacetonetriperoxide	na	223	na		
acetone	9.70 ± 0.01	58			
		15	14.41 ± 0.04	$C_6H_3^+ + CO + CH_3$	39
		43	10.49 ± 0.02	$CH_3CO^+ + CH_3$	39
			12.82 ± 0.03		39
		56	12.71 ± 0.03	$C_3H_4O^+ + H_2$	39
		57	13.10 ± 0.02	$C_3H_5O^+ + H$	39
hexane	10.13 ± 0.10	86			
		42	11.00 ± 0.035	$C_3H_6^+ + C_3H_8$	60
		43	11.33 ± 0.055	$C_3H_7^+ + C_3H_7$	60
		56	11.00 ± 0.015	$C_4H_8^+ + C_2H_6$	60
		57	11.03 ± 0.07	$C_4H_9^+ + C_2H_5$	60

[a] Data taken from the evaluated ionization potentials from ref 37. [b] na, data not available.

GC inlet. This allows for the delivery of a known concentration of analyte in the range of 1 part-per-million (ppm) to 1 part-per-billion (ppb) to the mass spectrometer. The permeation chamber was operated according to the manufacturer's procedure, and all the stainless steel transfer lines were heated (150 °C) to avoid the condensation of analytes on the walls. The carrier gas for all experiments was unfiltered laboratory air.

RESULTS AND DISCUSSION

SPI time-of-flight mass spectra have been obtained for the following species: NB, 1,3-DNB, o-NT, 2,4-DNT, 2,4,6-TNT, and TATP. In the situation when more than one isomer of the explosive, or ERC, exists, only the specified isomer was investigated. In addition, the SPI mass spectra of acetone and hexane were taken under the same conditions as those used to acquire the explosives mass spectra and used as verification that the dominant mechanism leading to ionization was indeed single (118.2 nm) photon absorption.

Table 1 presents the ionization energies (IE) and appearance energies (AE) for the molecules studied in this paper. The AE is defined as the minimum energy that must be imparted to an atom or molecule to produce a specified ion. Knowledge of the AE for specific product ions is used extensively in this study to characterize the ionization process and understand the mechanism by which certain species appear in the mass spectra.

VUV Source Characterization. In the case of nonresonant third harmonic generation, the third harmonic output power ($P_{3\omega}$), expected when a Gaussian beam of frequency ω is focused into an atomic medium is given by eq 1

$$P_{3\omega} = N^2|\chi^{(3)}(3\omega)|^2 P_\omega^3 F(b\Delta k) \quad (1)$$

where N is the number density of the gas, $\chi^{(3)}$ is the third-order nonlinear susceptibility of the medium, P_ω is the input power, and $F(b\Delta k)$ is the geometrical phase matching function where b is the confocal beam parameter and Δk is the wave vector mismatch.[26] Equation 1 predicts a VUV intensity linearly dependent on the cube of the input power $P\omega$ and was verified experimentally by measuring the NB ion signal as a function of input 354.6-nm power into the tripling cell, Figure 3. The slope of the logarithm of the NB ion signal versus the logarithm of the laser energy exhibits linearity up to 20 mJ input energy and then shows a rollover indicative of a decrease in conversion efficiency as the laser energy is increased up to the maximum energy of 46 mJ used in the experiment. The decrease in conversion efficiency is most probably due to laser-induced gas breakdown in the medium as the power density in the tripling volume increases. The linear region is best fit to a slope of 2.7 ± 0.1, indicating that the third harmonic generation is responsible for the ion signal. In addition, evacuation of the tripling cell results in the total loss of ion signal.

The molecules acetone (IE = 9.7 eV)[37] and hexane (IE = 10.13 eV)[37] were chosen as acceptable candidates for the characterization of the VUV source and verification of the ionization mechanism, as they have well-documented photochemistries and ionization energies below 10.49 eV. In addition, both molecules have

(37) Lias, S. G.; Bartmess, J. E.; Liebman, J. F.; Holmes, J. L.; Levin, R. D.; Mallard, W. D. In *NIST Chemistry WebBook, NIST Standard Reference Database Number 69*; Linstrom, P. J., Mallard, W. G., Eds.; National Institute of Standards and Technology: Gaithersburg, MD 20899, 2005; Vol. (http://webbook.nist.gov).

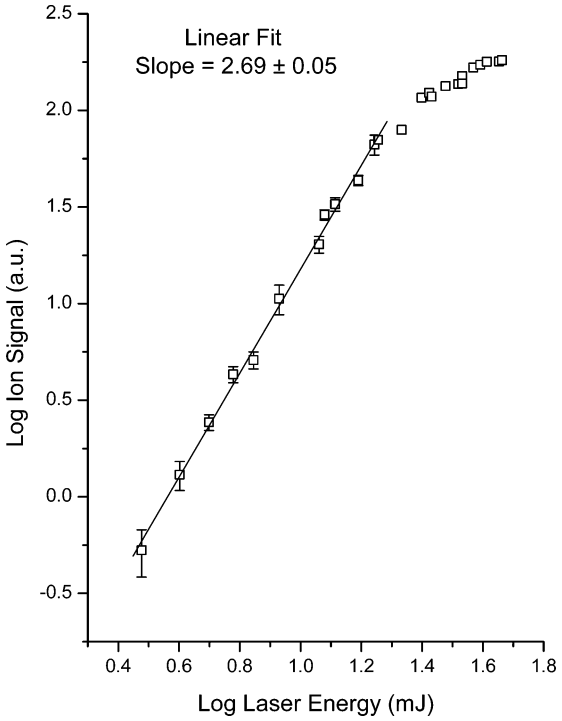

Figure 3. Plot of the logarithm of the ion signal versus the logarithm of the input laser energy to the tripling cell. The best fit to the linear portion of the data set yields a slope of 2.7 ± 0.1. The deviation from linearity in the ion signal at energies higher than 20 mJ is most likely due to laser-induced breakdown of the atomic gas medium as the power density in the tripling volume increases.

dissociation channels with energies lower than the 1 + 1 MPI(118.2 nm + 354.6 nm) threshold, yet higher than or equal to the single photon energy.

The mass spectra of acetone and hexane are shown in Figure 4A and B, respectively, and were taken under the same experimental conditions, used to acquire the TNT, ERCs, and TATP mass spectra. As can be seen in Figure 4, very little fragmentation of either species is observed. The most recent study of the VUV photoionization of acetone locates the thresholds for production of acetyl ion (43 amu) from neutral acetone at 10.49 ± 0.02 and 12.82 ± 0.03 eV.[38] In addition, the same study finds the threshold for production of $C_3H_4O^+$ (56 amu) and $CH_3COCH_2^+$ (57 amu) are 12.71 ± 0.03 and 13.10 ± 0.03 eV, respectively. A lack of the 56 and 57 amu ions in the SPI mass spectrum of acetone, in conjunction with a $43^+/58^+$ ratio lower than that shown in Figure 1 of Wei et al.[38] taken at 110 nm, provides direct evidence that SPI is the dominant ionization process.

A similar argument is made with hexane, Figure 4b. The appearance energies for fragment ions $C_3H_6^+$ (42 amu), $C_3H_7^+$ (43 amu), $C_4H_8^+$ (56 amu), and $C_4H_9^+$ (57 amu) from hexane are 11.00 ± 0.035, 11.33 ± 0.055, 11.00 ± 0.015, and 11.03 ± 0.07 eV, respectively.[39] Only very small contributions to the SPI mass spectrum from these fragment ions was found. Additionally, the SPI mass spectrum of hexane has previously been investigated and is found to be fragment free when the sample is at 20 °C.[40] The presented here are for 25 °C are in accord with this study.

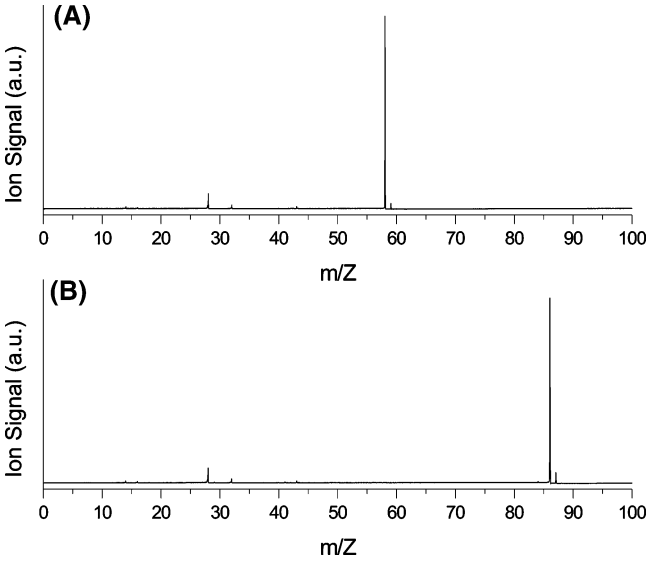

Figure 4. (A) Single photon ionization mass spectrum of acetone (MW = 58 amu). (B) Single photon ionization mass spectrum of hexane (MW = 86 amu). These species have well-documented photochemistries and are used as a verification that the dominant ionization mechanism is indeed from single photon ionization and not a higher energy 1 + 1 multiphoton process (118.2 + 354.6 nm).

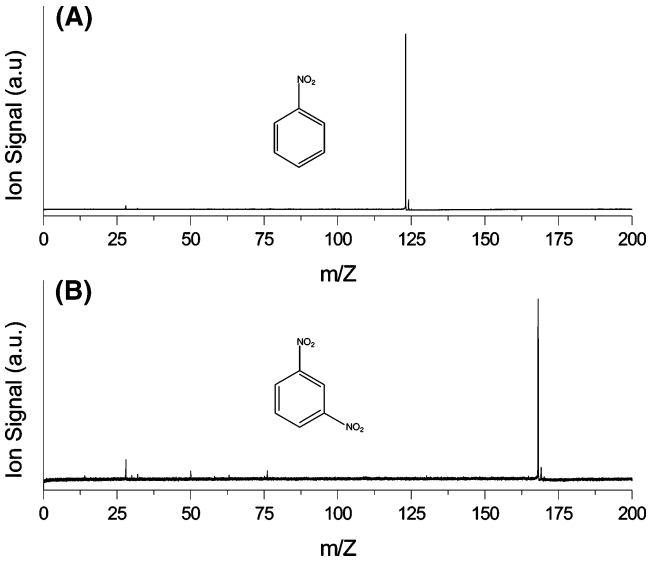

Figure 5. Single photon ionization mass spectrum of (A) nitrobenzene (MW = 123 amu) and (B) 1,3-dinitrobenzene (MW = 168 amu).

Nitrobenzene and 1,3-Dinitrobenzene. Figure 5 shows the mass spectra obtained from the single photon ionization of NB (IE = 9.94 eV)[37] and 1,3-DNB (IE = 10.4 eV).[37] The mass spectra of NB and 1,3-DNB are dominated by the parent peaks at 123 and 168 amu, respectively, with little fragmentation observed. The minor fragmentation observed for these species corresponds to $(M - NO_2)^+$ for NB and $(M - 2NO_2)^+$ for 1,3-DNB. Previous experimental work on NB including conventional mass spectrometry,[41–52] threshold photoelectron–photoion coincidence spectro-

(38) Wei, L. X.; Yang, B.; Yang, R.; Huang, C. Q.; Wang, J.; Shan, X. B.; Sheng, L. S.; Zhang, Y. W.; Qi, F.; Lam, C. S.; Li, W. K. *J. Phys. Chem. A* **2005**, *109*, 4231–4241.
(39) Steiner, B.; Giese, C. F.; Inghram, M. G. *J. Chem. Phys.* **1961**, *34*, 189–220.
(40) Steenvoorden, R.; Kistemaker, P. G.; Devries, A. E.; Michalak, L.; Nibbering, N. M. M. *Int. J. Mass Spectrom. Ion Processes* **1991**, *107*, 475–489.
(41) Brown, P. *Org. Mass Spectrom.* **1970**, *4*, 533–544.
(42) Brown, P. *Org. Mass Spectrom.* **1970**, *3*, 1175–1186.
(43) Beynon, J. H.; Bertrand, M.; Cooks, R. G. *J. Am. Chem. Soc.* **1973**, *95*, 1739–1745.

scopy,[53−55] and time-of-flight mass spectrometry in conjunction with synchrotron radiation,[56] has established the principal fragmentation pathways in the molecule and the energies at which they occur. For nitrobenzene, the dominant fragmentation pathways correspond to loss of NO and NO_2 resulting in $C_6H_5O^+$ (93 amu) and $C_6H_5^+$ (77 amu) product ions. The appearance energy for these species is reported to be 10.9 and 11.3 eV, respectively.[56] A 1 + 1 multiphoton absorption process (118.2 + 354.6 nm) in our experiments would correspond to ~14 eV of energy and would be sufficient for the creation of both product ion species. Relative abundance curve measurements, made by Cooper et al., as a function of photon energy for nitrobenzene reveal that at 14 eV of total energy the ratio of $C_6H_5^+$ (77 amu) to $C_6H_5O^+$ (93 amu) is roughly 6.7.[56] The presence of $C_6H_5^+$ is therefore thought to be the result of a 1 + 1 MPI process. Further, the absence of $C_6H_5O^+$ is most likely due to the low branching ratio for this channel at 14 eV and is thought to be below the threshold for detection under the experimental conditions. In addition, knowledge of the measured relative ion abundances for NB allows us to provide a more quantitative estimate of the ratio of MPI to SPI occurring from the VUV photon source. The ratio of the areas of $C_6H_5^+$ (77 amu) to $C_6H_5NO_2^+$ (123 amu) in Figure 5A, obtained by fitting the peak areas, is found to be 3×10^{-3}. This ratio, in conjunction with the relative abundance of $C_6H_5^+$ to $C_6H_5NO_2^+$ at 14 eV, 2.27, yields a value of $\sim 1.3 \times 10^{-3}$ for the ratio of MPI to SPI in these experiments.

Appearance energy measurements for 1,3-DNB are less abundant, and only the channel resulting in production of $C_6H_4NO_2^+$ (122 amu) has been measured using electron impact mass spectrometry and occurs at 12.3 eV.[41] The SPI mass spectrum of DNB (Figure 5B) lacks this peak, but does contain a minor contribution at 30, 50, and 76 amu. The mass 30, 50, and 76 amu peaks are most likely the NO^+, $C_4H_2^+$, and $(M - 2NO_2)^+$ species, respectively. PEPICO measurements on NB reveal the NO^+ loss channel to be a low-energy process occurring at 11.18 eV (IP NB = 9.94 eV),[53,54] and a similar situation may exist for 1,3-DNB.

***o*-Nitrotoluene and 2,4,-Dinitrotoluene.** The mass spectrum of *o*-NT (IE = 9.24 eV)[37] and DNT using the SPI-TOF-MS technique are presented in Figure 6. *o*-NT and 2,4-DNT also show dominant parent ion peaks at 137 and 182 amu, respectively. In contrast to the NB and 1,3-DNB, *o*-NT, and 2,4-DNT show strong fragment peaks corresponding to the loss of $(M - OH)^+$ for both species, resulting in mass peaks at 120 and 165 amu. Hydroxyl loss from o-NT is well documented, and the appearance energy for $C_7H_6NO^+$ is 9.69 eV.[57] At 10.49 eV, there is enough energy to both photoionize and dissociate *o*-NT. An additional dissociation channel resulting in the loss of $(M - NO_2)^+$ occurs at 11.0 eV[37] but is not observed in the mass spectra presented here of these molecules to an appreciable extent. To the best of our knowledge, there is no known measurement of the ionization energy of 2,4-DNT. The observed parent ion signal for 2,4-DNT indicates that the ionization energy of 2,4-DNT is below the photon energy of 10.49 eV.

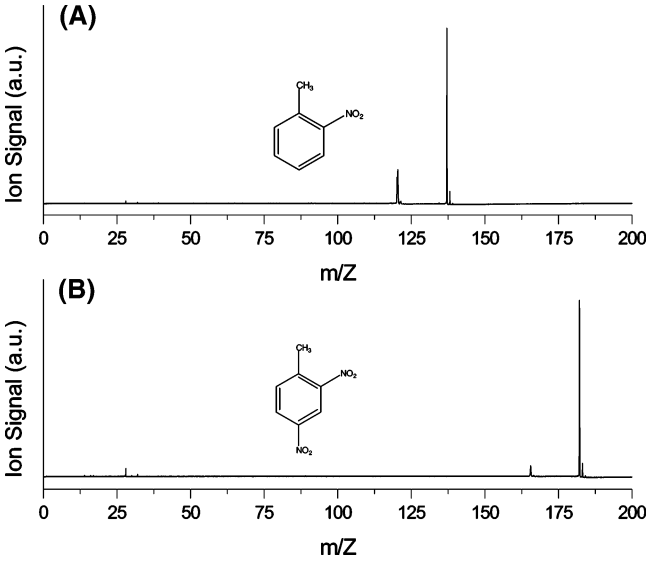

Figure 6. (A) Single photon ionization mass spectrum of *o*-nitrotoluene (MW = 137 amu). The mass spectrum consists of the parent molecular ion and hydroxyl loss $(M - OH)^+$ species (120 amu). (B) Single photon ionization mass spectrum of 2,4-dinitrotoluene, consisting of the parent ion and hydroxyl loss species $(M - OH)^+$ (165 amu).

2,4,6-Trinitrotoluene. Figure 7 shows the SPI-TOF mass spectrum of 2,4,6-TNT. The mass spectrum consists of the parent peak at 227 amu and the $(M - OH)^+$ product ion at 210 amu. Figure 7B is an expanded view of the mass spectrum in the parent ion region and is included to demonstrate the mass resolution and S/N ratio in this region. Again, to the best of our knowledge, only one published value for the ionization energy of 2,4,6-TNT using photoionization mass spectrometry (10.59 ± 0.04 eV)[58] exists, and no values could be found regarding the appearance energies for this molecule. The presence of the parent ion signal indicates that an upper bound for the ionization energy for 2,4,6-TNT is 10.49 eV. One possible explanation for the discrepancy in the two measurements is that the current measurement is made by heating the 2,4,6-TNT sample and capillary introduction system to 150 °C. The added thermal energy could potentially lead to parent ion generation at longer wavelengths. Such an effect has been observed previously.[40]

(44) Jones, E. G.; Bauman, L. E.; Beynon, J. H.; Cooks, R. G. *Org. Mass Spectrom.* **1973**, *7*, 185−192.
(45) McLafferty, F. W.; Bente, P. F.; Kornfeld, R.; Tsai, S. C.; Howe, I. *J. Am. Chem. Soc.* **1973**, *95*, 2120−2129.
(46) Matyuk, V. M.; Potapov, V. K.; Prokhoda, A. L. *Zh. Fizicheskoi Khim.* **1979**, *53*, 957−962.
(47) Proctor, C. J.; Kralj, B.; Brenton, A. G.; Beynon, J. H. *Org. Mass Spectrom.* **1980**, *15*, 619−631.
(48) Porter, C. J.; Beynon, J. H.; Ast, T. *Org. Mass Spectrom.* **1981**, *16*, 101−114.
(49) Griffiths, I. W.; Mukhtar, E. S.; Harris, F. M.; Beynon, J. H. *Int. J. Mass Spectrom. Ion Processes* **1981**, *38*, 333−342.
(50) Allam, S. H.; Migahed, M. D.; Khodary, A. E. *Int. J. Mass Spectrom. Ion Processes* **1981**, *39*, 117−122.
(51) Kingston, E. E.; Morgan, T. G.; Harris, F. M.; Beynon, J. H. *Int. J. Mass Spectrom. Ion Processes* **1983**, *47*, 73−76.
(52) Hwang, W. G.; Kim, M. S.; Choe, J. C. *J. Phys. Chem.* **1996**, *100*, 9227−9234.
(53) Panczel, M.; Baer, T. *Int. J. Mass Spectrom. Ion Processes* **1984**, *58*, 43−61.
(54) Nishimura, T.; Das, P. R.; Meisels, G. G. *J. Chem. Phys.* **1986**, *84*, 6190−6199.
(55) Bunn, T. L.; Richard, A. M.; Baer, T. *J. Chem. Phys.* **1986**, *84*, 1424−1431.
(56) Cooper, L.; Shpinkova, L. G.; Rennie, E. E.; Holland, D. M. P.; Shaw, D. A. *Int. J. Mass Spectrom.* **2001**, *207*, 223−239.
(57) Shao, J. D.; Baer, T. *Int. J. Mass Spectrom. Ion Processes* **1988**, *86*, 357−367.
(58) Potapov, V. K.; Kardash, I. E.; Sorokin, V. V.; Sokolov, S. A.; Evlasheva, T. I. *High Energy Chem.* **1972**, *6*, 347−349.

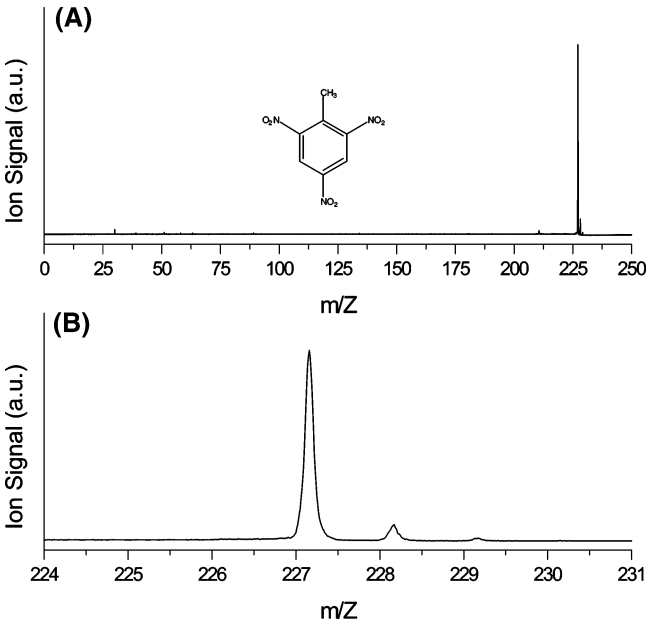

Figure 7. (A) 2,4,6-Trinitrotoluene single photon ionization mass spectrum. (B) Expanded view of the parent molecular ion region.

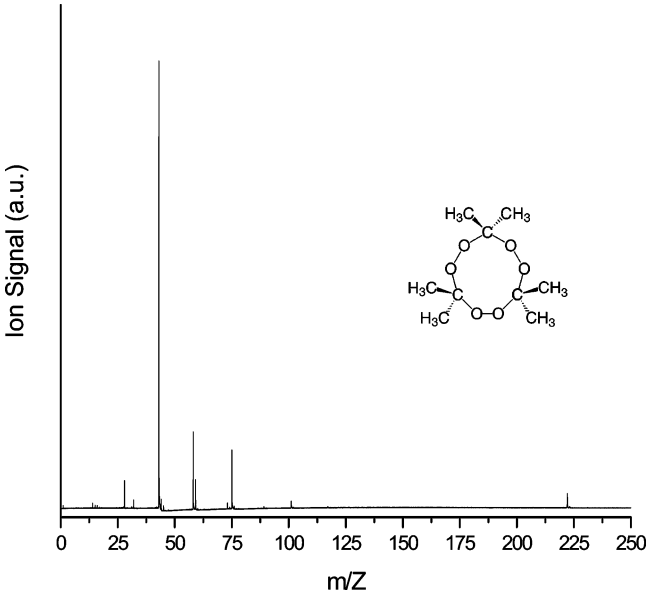

Figure 8. Single photon ionization mass spectrum of triacetone triperoxide (MW = 223 amu).

Triacetone Triperoxide. The prospect of applying this technique to the detection of peroxide-based explosives was also evaluated. Figure 8 is the mass spectrum of TATP taken with SPI. In contrast to the nitro-based explosives and ERCs, TATP exhibits extensive fragmentation. The parent molecular ion (222 amu) is present in addition to a number of photodissociative product species including acetyl ion (43 amu), acetone ion (58 amu), $C_3H_7O^+$ (59 amu), $C_3H_7O_2^+$ (75 amu), $C_3H_6O_4^+$ (106 amu), and diacetone diperoxide $C_3H_6O_5^+$ (122 amu). The SPI-TOF-MS of TATP is found to be qualitatively similar to the EI mass spectrum[59,60] as well as the femtosecond laser photoionization

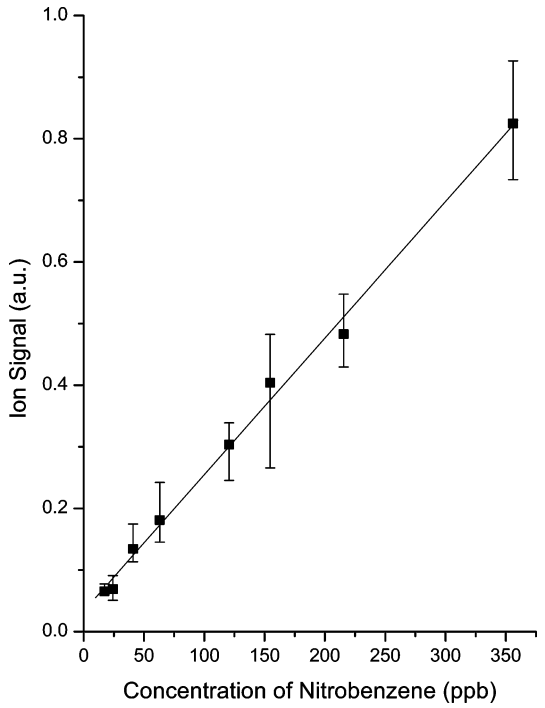

Figure 9. Nitrobenzene calibration curve used to determine the LOD for the SPI TOF technique. The limit of detection was determined at a S/N ratio of 2:1 and is 17−24 ppb for nitrobenzene.

mass spectrum taken at 795 nm with 130-fs pulses.[61] The latter techniques often result in extensive fragmentation of the explosives and ERCs due to the high energy of the ionizing electron in the case of EI or the rapid nature of the fragmentation mechanisms, which the ultrafast laser pulse can only partially overcome. We are confident that the TATP mass spectrum is obtained under SPI conditions and that the extensive fragmentation observed is due to photophysical processes occurring in the molecule rather than resulting from a high-energy MPI process. It appears that the 10.49-eV photon energy is in excess of the AE for dissociative photoionization.

Limits of Detection. The LODs for NB and 2,4-DNT using SPI were also measured. Using the permeation device described previously, the LOD for both NB and 2,4-DNT were determined to be 17−24 (S/N ∼ 2:1) and ∼40 ppb (S/N ∼ 2:1), respectively. Figure 9 presents the calibration curve for the NB sensitivity measurements and shows a linear instrument response over 1 order of magnitude in concentration. Sensitivity measurements were conducted by averaging 300 laser shots, with 30 mJ of 354.6-nm energy impingent on the SPI cell. The S/N ratio was estimated by visual inspection of the mass spectrum. The ppb-level sensitivity of this method is comparable to sensitivity measurements that were previously reported for the nanosecond REMPI-LIF studies of similar compounds.[15,16,20]

To demonstrate the feasibility of the presented approach, the determined detection limits were compared with known vapor pressures of some explosives at ambient temperatures.[62−64] As can be seen in Table 2 the vapor pressures for explosives of interest

(59) Stambouli, A.; El Bouri, A.; Bouayoun, T.; Bellimam, M. A. *Forensic Sci. Int.* **2004**, *146*, S191−S194.
(60) Muller, D.; Levy, A.; Shelef, R.; Abramovich-Bar, S.; Sonenfeld, D.; Tamiri, T. *J. Forensic Sci.* **2004**, *49*, 935−938.
(61) Mullen, C.; Huestis, D. L.; Coggiola, M. J.; Oser, H. *Int. J. Mass Spectrom.* In press.
(62) Steinfeld, J. A.; Wormhoudt, J. *Annu. Rev. Phys. Chem.* **1988**, *49*, 203−232.
(63) Pella, P. A. *J. Chem. Thermodyn.* **1977**, *9*, 301−305.
(64) Moore, D. S. *Rev. Sci. Instrum.* **2004**, *75*, 2499−2512.

Table 2. Room-Temperature Vapor Pressures of Selected Explosives and ERCs

molecule	vapor pressure (Torr) at 25 °C	concn (ppb)	ref
triacetonetriperoxide	0.5	60 000	62
nitroglycerine	6.1×10^{-4}	740	64
2,4-dinitrotoluene	1.4×10^{-4}	170	63
2,4,6-trinitrotoluene	8.0×10^{-6}	10	64
RDX	4.0×10^{-9}	0.008	62

span 7 orders of magnitude. However, except for RDX with an exceptionally low vapor pressure, all the explosives and ERCs including TNT could arguably present sufficient vapor to measure in real time with the presented single photon ionization approach if a robust sampling system were employed.

CONCLUSION

We have demonstrated that a plausible approach to laser-based detection of explosives is the use of SPI, where one photon directly ionizes the explosives or ERCs to produce parent ions in a single step. The energetics associated with SPI achieves a degree of chemical selectivity by allowing for the detection of the parent molecular ion in the presence of little or no fragmentation.This is in contrast to nanosecond REMPI TOF-MS, which produes only the NO^+ moiety.

A potential drawback to the 118.2-nm SPI method is its applicability to only those molecules with ionization energies below 10.49 eV. However, our results indicate that parent ions of NB, 1,3-DNB, *o*-NT, 2,4-DNT, 2,4,6-TNT, and to a lesser extent TATP can be generated using the SPI-TOF-MS technique.

We have found that SPI of the nitro-containing explosives yields mass spectra of these species that are dominated by the parent molecular ion. In addition, in cases where the AE of a particular ionic species from the parent molecule is below the photon energy used, the fragment is observed. The ortho-substituted nitrotoluenes manifested this effect to the greatest extent, and the fragments observed are understood to occur as a result of hydroxyl (OH) loss from the parent species upon ionization.

In contrast, the peroxide-based explosive TATP, while successfully observed with SPI, undergoes extensive fragmentation, and is though to be a result of the photophysical processes of the molecule.

Based on these results, future work will include SPI experiments on other explosives and ERCs, including accurate sensitivity measurements on additional species that will determine the applicability of this technique to explosives detection.

ACKNOWLEDGMENT

This material is based upon work supported by the National Science Foundation under Grant CHE-0321288. The authors also acknowledge the support by a subaward agreement from The Johns Hopkins University with funds provided by Grant No. DAAD 19-02-1-0255 from U.S. Army Robert Morris Acquisition. B.V.P. acknowledges Stanford University for funding her research at SRI International. A.I. acknowledges the NSF-Research Experience for Undergraduate (REU) Program for funding. The authors also thank Jeffrey Bottaro for the synthesis of the TATP samples.

Received for review January 27, 2006. Accepted March 27, 2006.

AC060190H